Doppler-free spectroscopy of the Cs $6S_{1/2} - 7P_{3/2}$ atomic transition at 456 nm in a nanometric-thick vapor layer

ARMEN SARGSYAN[1], EMMANUEL KLINGER[2,*], RODOLPHE BOUDOT[2], AND DAVID SARKISYAN[1]

[1] Institute for Physical Research – National Academy of Sciences of Armenia, 0204 Ashtarak-2, Armenia
[2] Université Marie et Louis Pasteur, SUPMICROTECH, CNRS, Institut FEMTO-ST, F-25000 Besançon, France
[*] Corresponding author: emmanuel.klinger@femto-st.fr

Compiled April 15, 2025

The features of Doppler-free resonances detected by probing the ^{133}Cs atom $6S_{1/2} - 7P_{3/2}$ transition at 456 nm in a nanometric-thick vapor layer are investigated. The matrix element of this transition is about 11 times smaller than that of the Cs D_2 line (852 nm). When the vapor layer thickness is $\ell = \lambda/2 \simeq 230$ nm, we observe Dicke narrowing of the lines, accompanied by a red frequency shift of the atomic transitions, which is attributed to atom-surface interactions. Realizing optical pumping with $\ell \simeq 460$ nm in a single-pass configuration, we observe Doppler-free resonances with a linewidth < 20 MHz, located at the atomic transitions frequencies with a correspondence of the amplitudes to the transition intensities. These narrow resonances are of interest for high-resolution spectroscopy and instrumentation, and could serve as a frequency reference.

http://dx.doi.org/10.1364/ao.XX.XXXXXX

Many contemporary optics and atomic physics experiments are realized using alkali vapors such as Rb and Cs. Spectroscopy of hot vapors [1] is at the core of many devices and applications, such as atomic optical clocks and gyroscopes [2], optical magnetometers [3], Faraday filters [4], or light-trapping experiments with electromagnetically induced transparency [5]. Typically, the transitions used in these experiments are the D_1 and D_2 lines, resonant with near-infrared light (600 – 900 nm).

Probing higher-frequency transitions in cesium with sub-Doppler spectroscopy has recently attracted interest as these transitions could serve as optical frequency references [6, 7]. Nevertheless, the literature on high resolution spectroscopy of the $7P_J$ states of ^{133}Cs is scarce. The Cs $6S_{1/2} \rightarrow 7P_J$ transitions were investigated for both $J = 1/2$ (459 nm) and $J = 3/2$ (456 nm) to precisely measure their matrix element [8] and their lifetime [9]. A study of nonlinear magneto-optical resonances observed in the fluorescence to the ground state from the $7P_{3/2}$ state, populated by direct optical pumping with a laser radiation at 456 nm, was carried out in Ref. [10]. In Ref. [11], the $6S_{1/2} \rightarrow 7P_{3/2}$ transitions were studied using the well-known saturated absorption (SA) technique, enabling sub-Doppler resolution of these transitions.

As was thoroughly studied on alkali D lines, see e.g. Refs. [12–15], and even some molecular lines [16, 17], probing resonances in vapor layers having a thickness on the order of the excitation wavelength offers an alternative to usual sub-Doppler spectroscopy achieved with nonlinear processes. One advantage is that light-matter interaction occurs in the weak-probe regime, simplifying both the experimental setup and the interpretation of results. In these cells, referred to as nanocells (NC), the narrowest transmission spectra are obtained at two preferred thicknesses: $\ell = \lambda/2$ and $\ell = \lambda$, where λ is the wavelength of laser radiation that is resonant with the corresponding transition. In the first case ($\ell = \lambda/2$), both the transmission and fluorescence spectra exhibit a significant sub-Doppler narrowing (by factors of three and six, respectively) compared to centimeter-sized vapor cells [13, 14]. The second case ($\ell = \lambda$) is characterized by the possibility of forming narrow resonances by means of velocity-selective optical pumping (VSOP), located at atomic transitions, in the transmission spectrum [18]. To allow for the study of atomic resonances as a function of the thickness ℓ of the vapor layer (transverse to the laser beam), our NCs are fabricated with a wedge gap between their windows, in the vertical direction [19]. In this way, the required thickness is achieved either via mechanical movement of NC or via spatial translation of the laser beam.

In this work, we perform qualitative Doppler-free spectroscopy of the ^{133}Cs $6S_{1/2} \rightarrow 7P_{3/2}$ transition at $\lambda = 455.6$ nm in a nanometric thick vapor layer, contained in a NC. One of the challenges is that the $6S_{1/2} \rightarrow 7P_{3/2}$ transition has a dipole moment about 11 times smaller than that of the D_2 line [8], and, together with the small optical path of the NC, makes the recording of spectral features challenging. This issue is addressed by increasing the temperature of the NC to about 180°C where it would usually be set to about 120°C in the case of alkali D lines. The spectra obtained for $\ell = \lambda/2$ and $\ell = \lambda$ are compared with that obtained with saturated absorption spectroscopy from a cm-long vapor cell. When $\ell = \lambda/2$, we show that the Dicke narrowing is accompanied by a 35 MHz-large red frequency shift and broadening of the atomic transitions due to atom-surface interactions, negligible at this scale in the case of D lines. This

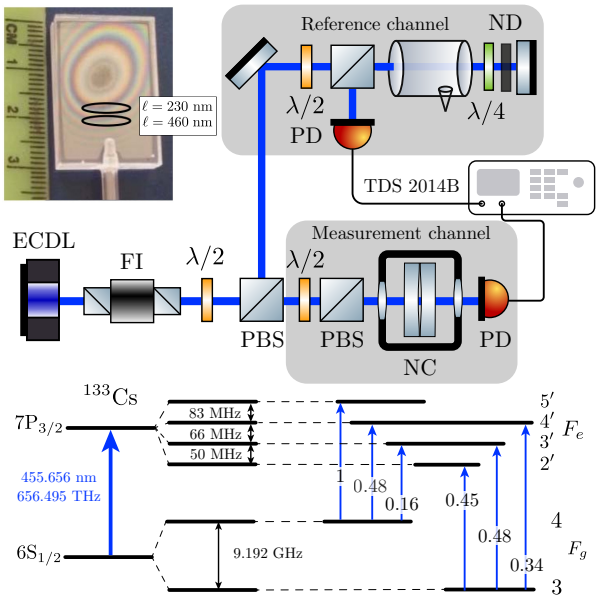

Fig. 1. (top) Sketch of the experimental setup. ECDL – external cavity diode laser; FI – Faraday isolator; PBS – Glan polarizer; NC – nanocell containing Cs atomic vapor, placed inside the heater; PD–photodetectors. The signals are proceeded by a digital storage oscilloscope. The frequency reference is realized with saturated absorption spectroscopy. The inset shows a photograph of the NC filled with Cs where the upper and lower ovals mark the thickness $\ell \sim 230$ nm and $\ell \sim 460$ nm. (bottom) Energy levels involved in the $6S_{1/2} \rightarrow 7P_{3/2}$ transitions. The relative frequency shifts are indicated between hyperfine levels, together with the transition intensities, normalized to the largest one: $F_g = 4 \rightarrow F_e = 5$.

makes wedged NCs a platform of choice to perform quantitative studies of atom-surface interactions. We also show that the thickness $\ell = \lambda$ is preferred to perform high-resolution spectroscopy. In this case, the second derivative [20] of the spectra exhibits sub 20 MHz-wide Doppler-free resonances not affected by atom-surface interactions.

The experimental setup is sketched in Fig. 1. A tunable external-cavity diode laser (ECDL) with a spectral linewidth of about 400 kHz is tuned in the vicinity of the $6S_{1/2} \rightarrow 7P_{3/2}$ transitions ($\lambda = 456$ nm) of Cs atoms. The laser beam is directed at normal incidence onto the windows of a NC containing Cs atomic vapor. The NC is placed in an oven to adjust the temperature to about $T \approx 180°$C, corresponding to a vapor number density of about 5.5×10^{14} cm^{-3}. The vapor column thickness is adjusted by translation of the nanocell-oven assembly. The thickness of atomic vapor column $\ell \approx \lambda/2$ or $\ell \approx \lambda$ are marked on the top left inset in Fig. 1. The details of the NC design can be found in Ref. [19]. The light transmitted through the NC is recorded using photodiodes, and their signals are fed into a digital storage oscilloscope. A fraction of the light is used to make a frequency reference channel based on saturated absorption in a cm-long glass-blown Cs cell.

Figure 2 shows the features of the transmission spectrum for thicknesses $\ell \approx \lambda/2$ and $\ell \approx \lambda$. Figure 2(a) shows the transmission spectrum of the $F_g = 4 \rightarrow F_e = 3, 4, 5$ manifold (hereafter, the notation is simplified to $F = 4 \rightarrow 3', 4', 5'$), while Fig. 2(b) shows the transmission spectrum of the $F = 3 \rightarrow 2', 3', 4'$ manifold. These transitions are indicated by vertical dashed lines. The energy level diagram, showing the transitions and their intensities, is presented at the bottom of Fig. 1.

The top panels in Fig. 2 show the transmission spectra obtained with $\ell \approx \lambda/2$ and a laser power of about 0.2 mW. In this case, the spectra exhibit a significant narrowing, referred to as Dicke narrowing: the transmitted spectra are typically about four times narrower in comparison with the Doppler linewidth [13, 14]. Here, the transitions are, in addition, seen to be shifted by about 35 MHz toward lower frequencies with respect to the non-shifted atomic transitions. This is caused by van der Waals (vdW) interaction (also known as Casimir-Polder interaction in the non-retarded regime) between Cs and the technical sapphire windows of the NC, evidence of atom-surface interaction [21–24]. This is characterized by a broader, asymmetric atomic lineshape whose center experiences a red frequency shift. To estimate the red frequency shift in an NC, one can use the formula [20]

$$\Delta\nu_{\mathrm{vdW}} = -16C_3/\ell^3, \qquad \textbf{(1)}$$

giving the shift in the middle of the cell, where C_3 is a coupling constant that depends on the surface and the atomic state. For alkali D lines interacting with sapphire, one typically has $C_3 \sim 1-2$ kHz μm^3. For this reason, the vdW interaction causes a red frequency shift typically observable for $\ell < 100$ nm [25]. It is known, however, that the atomic polarizability, linked to the C_3 coefficient of vdW effect, is increasing with the principal quantum number n [23, 26]. Indeed, we measure $\Delta\nu_{\mathrm{vdW}} \sim 35$ MHz for the $6S_{1/2} \rightarrow 7P_{3/2}$ transition at $\ell \simeq 230$ nm, yielding $C_3 \sim 20$ kHz μm^3. This is in good agreement with the value presented in Ref. [27]. Note that these measurements are sensitive to the spectroscopic C_3 coefficient (i.e. the difference between excited and ground state coefficients).

The gray-filled curves in the top panels of Fig. 2 are theoretical spectra calculated following the approach described in Ref. [12] with $\Gamma/2\pi = 40$ MHz and $\ell = 230$ nm. Here, we have taken into account the van der Waals shift, given by Eq. (1). Note, however, that the red frequency shift due to AS interaction is accompanied by a distortion of the atomic resonance profile, which we do not take into account. This explains the discrepancies observed between experiments and theory.

Middle panels in Fig. 2 show transmission spectra obtained for $\ell \simeq 460$ nm and a laser power of about 1 mW. It contains six VSOP resonances (three for each ground state manifold) located at the corresponding transitions. The VSOP resonance linewidth (FWHM) is measured to be 28 MHz, which accounts for the natural linewidth $\Gamma_N/2\pi \approx 1.16$ MHz of the $7P_{3/2}$ level [9] and some residual Doppler width. To estimate the VSOP linewidth, one can use the simple formula

$$\Gamma_{VSOP} = \sqrt{\Gamma_D \times \Gamma_N} \approx 2\pi\ 32\ \mathrm{MHz}. \qquad \textbf{(2)}$$

Note that VSOP resonances can appear in the transmission spectrum obtained from a nanocell with thicknesses $\ell = m\lambda$, where m is an integer. However, with increasing m, a spectral broadening occurs.

In comparison, the bottom panels in Fig. 2 show the saturation absorption spectrum obtained with a 1-cm long Cs vapor cell heated to about 80°C. For each ground state manifold, it contains three VSOP resonances and three crossover (CO) resonances, typical of saturated absorption. Here, the transitions overlap because of the presence of CO resonances, often more intense than the transitions themselves. Meanwhile, the transitions are very well spectrally resolved in the case of the NC.

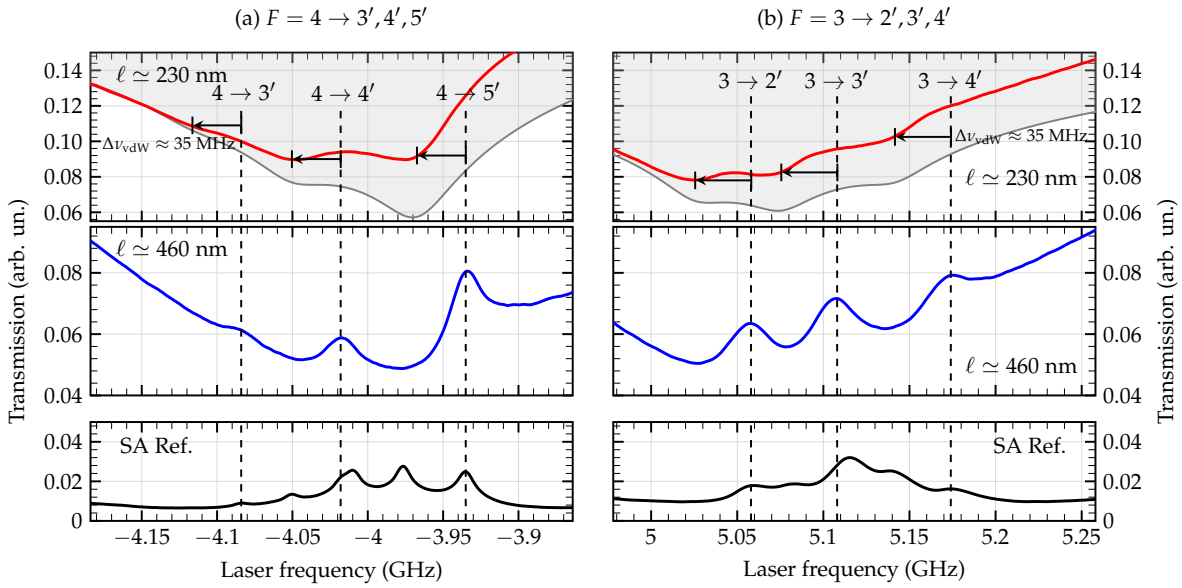

Fig. 2. Transmission spectra of the $6S_{1/2} \rightarrow 7P_{3/2}$ transition at 455.6 nm for (a) the $F = 4 \rightarrow 3', 4', 5'$ manifold and (b) the $F = 3 \rightarrow 2', 3', 4'$ manifold. The top panels show the transmission spectra obtained for a vapor layer thickness of $\ell \simeq 230$ nm and a laser power of about 0.2 mW. A 35 MHz-large red frequency shift of the atomic transitions with respect to the unperturbed transitions marked by dashed lines is observed. This shift is attributed to atom-surface interaction [21]. The gray-filled curves are the theoretical spectra calculated for $\ell = 230$ nm with $\Gamma = 40$ MHz, taking into account Eq. (1), see text. The middle panels show the transmission spectra obtained with $\ell \simeq 460$ nm, which contains six VSOP resonances (three for each manifold) not shifted by atom-surface interaction, with a linewidth of about 28 MHz. These are obtained by increasing the laser power to about 1 mW. The bottom panels show spectra obtained with saturated absorption from a cm-long glass-blown vapor cell. The six VSOP resonances, marked by vertical dashed lines, are seen to partially overlap with six CO resonances. The zero laser frequency corresponds to the weighted center of the $6S_{1/2} \rightarrow 7P_{3/2}$ transition. Note that the peak transmission in the case of the NC is 99% while it is about 85% in the case of the cm-long cell.

Moreover, the amplitudes of the resonances correspond to the transition intensities, see Fig. 1. Thus, VSOP resonances obtained from a NC with $\ell \approx \lambda$ appear promising to serve as a frequency reference tool.

As was shown in [20], the second derivative (SD) technique can be employed to further narrow the atomic lines. It can be done through either digital processing (for example, with a frequency modulation technique) of the recorded transmission trace or by numerical processing with a computer. Figure 3 shows the curves of the middle and bottom panels of Fig. 2 processed with second derivative. In the case of the NC (top panels), the transition linewidth in the SD spectrum is seen to reduce down to about 15 MHz, that is a 58-fold narrower as compared with the Doppler width ($\Gamma_D/2\pi \approx 0.87$ GHz at 180°C). A similar value is obtained in Ref. [7] using SA technique with two counter-propagating laser beams in a 1.4-mm long microfabricated Cs cell. Here, these narrow resonances are obtained in a single-pass configuration. Note that the SD treatment of signals recorded with NCs preserves not only the frequency positions of the spectral features but also their amplitudes linked to the transition probabilities. Thus, the narrow VSOP resonances obtained with the NC at $\ell \approx 460$ nm are of interest for high-resolution spectroscopy and instrumentation. The bottom panels in Fig. 3 show, for comparison, the SA transmission spectrum also processed with SD. Despite being narrower, spectral features corresponding to atomic transitions are still partially overlapped with CO resonances. That is especially the case for transitions $F = 4 \rightarrow 4'$ [Fig. 3(a)] and $F = 3 \rightarrow 3'$ [Fig. 3(b)].

The advantages of sub-Doppler spectroscopy using NCs as a frequency reference tool are as follows: (i) simplicity of the realization geometry (single-beam transmission as opposed to counter-propagating beams requirement for SA geometry); (ii) low value of the required laser power (typically a factor of ten less than that needed for the SA technique); (iii) absence of CO resonances, which is especially important for example when atomic transitions are studied in an external field, since this leads to the splitting of the CO resonances into a large number of additional components; (iv) correspondence of the amplitudes of atomic resonances to their corresponding transition intensities. Finally, it is important to note that achieving a precise NC thickness of $\ell = \lambda/2$ or $\ell = \lambda$ is not crucial: narrow spectra are observed within a tolerance of $\Delta\ell = \pm 30$ nm, which makes the proposed technique experimentally feasible. Note that laser frequency stabilization using a NC with thickness $\ell \approx \lambda/2$ has been demonstrated in Ref. [28].

In conclusion, we have performed high-resolution spectroscopy of the $6S_{1/2} \rightarrow 7P_{3/2}$ transitions at 455.6 nm in a Cs vapor nanolayer. We have observed that the Dicke narrowing of the spectrum at $\ell = \lambda/2 \simeq 230$ nm is accompanied by a red frequency shift due to atom-surface interactions. This makes wedged NCs a platform of choice to perform quantitative studies of atom-surface interactions. Note that Dicke-narrowed resonances with minimized impact from atom-surface interactions should be observed for $\ell \approx 3\lambda/2 \approx 680$ nm albeit with a Doppler pedestal [13]. This will be subject to future investigations. In addition, the resonances formed using a NC with $\ell = \lambda \simeq 460$ nm and VSOP, experience a 50-fold spectral narrowing with respect to the Doppler broadened Cs atomic lines.

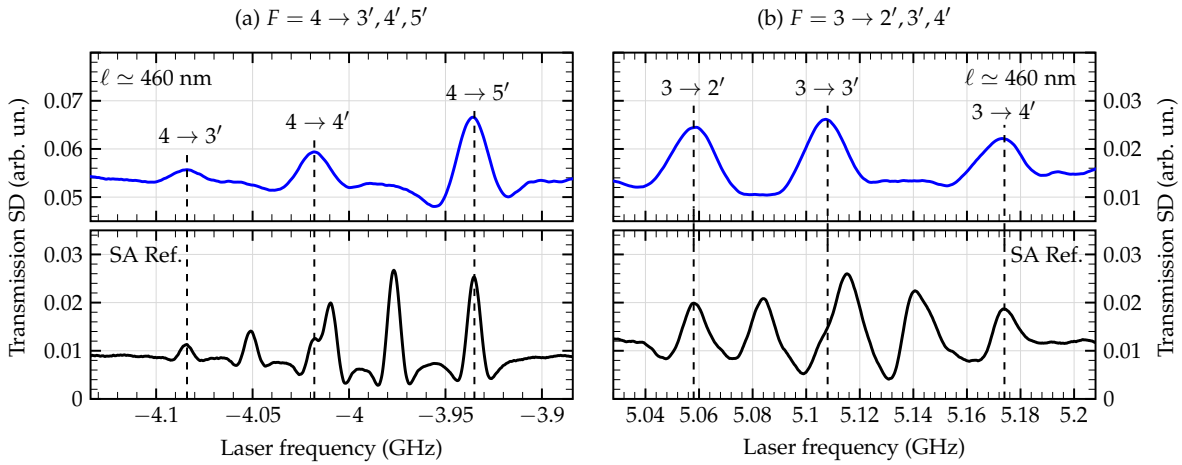

Fig. 3. Second derivative transmission spectra of the $6S_{1/2} \to 7P_{3/2}$ transition at 455.6 nm for (a) the $F = 4 \to 3', 4', 5'$ manifold and (b) the $F = 3 \to 2', 3', 4'$ manifold. The top panels show the SD spectra obtained after processing the raw transmission spectra recorded from a vapor layer of thickness $\ell \simeq 460$ nm (middle panels in Fig. 2). The bottom panels show the SD spectra obtained by processing the SA reference spectrum (bottom panels in Fig. 2). All of these demonstrate a better spectral resolution than the raw transmission spectra.

This last result could be useful to investigate the evolution of the transitions in a magnetic field. One expects to observe, for example, magnetically-induced transitions [29]: five transitions for the $F = 4 \to 2'$ manifold and seven for the $F = 3 \to 5'$ manifold of the $6S_{1/2} \to 7P_{3/2}$ transition.

We also expect that Cs NCs could be successfully used in the spectroscopy of $6S_{1/2} \to 7P_{1/2}$ (459 nm) $6S_{1/2} \to 8P_{3/2}$ spectroscopy (388 nm). Note that the recent development of a glass NC [30], which is easier to manufacture than sapphire-made NC used in the present work, could make the nanocells available for a wider range of researchers.

FUNDING

AS and DS acknowledge support Higher Education and Science Committee of RA in the frame of the research project n°25RG-1C008. EK and RB acknowledge support from Agence Nationale de la Recherche (EIPHI Graduate school grant ANR-17-EURE-0002); Région Bourgogne Franche-Comté.

DISCLOSURES

The authors declare no conflicts of interest.

DATA AVAILABILITY STATEMENT

The data that support the findings of this study are available from the corresponding author upon reasonable request.

REFERENCES

1. D. Pizzey, J. D. Briscoe, F. D. Logue, *et al.*, New J. Phys. **24**, 125001 (2022).
2. J. Kitching, Appl. Phys. Rev. **5**, 031302 (2018).
3. A. Fabricant, I. Novikova, and G. Bison, New J. Phys. **25**, 025001 (2023).
4. D. Uhland, H. Dillmann, Y. Wang, and I. Gerhardt, New J. Phys. **25**, 125001 (2023).
5. R. Finkelstein, S. Bali, O. Firstenberg, and I. Novikova, New J. Phys. **25**, 035001 (2023).
6. J. Miao, T. Shi, J. Zhang, and J. Chen, Phys. Rev. Appl. **18**, 024034 (2022).
7. E. Klinger, A. Mursa, C. M. Rivera-Aguilar, *et al.*, Opt. Lett. **49**, 1953 (2024).
8. A. Damitz, G. Toh, E. Putney, *et al.*, Phys. Rev. A **99**, 062510 (2019).
9. G. Toh, N. Chalus, A. Burgess, *et al.*, Phys. Rev. A **100**, 052507 (2019).
10. M. Auzinsh, R. Ferber, F. Gahbauer, *et al.*, Opt. Commun. **284**, 2863 (2011).
11. F. Li, B. Zhao, J. Wei, *et al.*, Opt. Lett. **44**, 3785 (2019).
12. G. Dutier, S. Saltiel, D. Bloch, and M. Ducloy, J. Opt. Soc. Am. B **20**, 793 (2003).
13. G. Dutier, A. Yarovitski, S. Saltiel, *et al.*, Europhys. Lett. **63**, 35 (2003).
14. D. Sarkisyan, T. Varzhapetyan, A. Sarkisyan, *et al.*, Phys. Rev. A **69**, 065802 (2004).
15. A. Sargsyan, G. Hakhumyan, A. Papoyan, *et al.*, Appl. Phys. Lett. **93**, 021119 (2008).
16. J.-M. Hartmann, X. Landsheere, C. Boulet, *et al.*, Phys. Rev. A **93**, 012516 (2016).
17. G. G. Arellano, J. C. de Aquino Carvalho, H. Mouhanna, *et al.*, Nat. Commun. **15**, 1862 (2024).
18. S. Briaudeau, D. Bloch, and M. Ducloy, Europhys. Lett. (EPL) **35**, 337–342 (1996).
19. J. Keaveney, A. Sargsyan, U. Krohn, *et al.*, Phys. Rev. Lett. **108**, 173601 (2012).
20. A. Sargsyan, A. Amiryan, Y. Pashayan-Leroy, *et al.*, Opt. Lett. **44**, 5533 (2019).
21. A. Laliotis, B.-S. Lu, M. Ducloy, and D. Wilkowski, AVS Quantum Sci. **3** (2021).
22. M. Chevrollier, D. Bloch, G. Rahmat, and M. Ducloy, Opt. Lett. **16**, 1879 (1991).
23. A. Sargsyan, R. Momier, C. Leroy, and D. Sarkisyan, Phys. Lett. A **483**, 129069 (2023).
24. B. Dutta, J. C. d. A. Carvalho, G. Garcia-Arellano, *et al.*, Phys. Rev. Res. **6**, L022035 (2024).
25. T. Peyrot, N. Šibalić, Y. R. P. Sortais, *et al.*, Phys. Rev. A **100**, 022503 (2019).
26. C. S. Adams, J. D. Pritchard, and J. P. Shaffer, J. Phys. B: At. Mol. Opt. Phys. **53**, 012002 (2019).
27. J. C. de Aquino Carvalho, I. Maurin, P. Chaves de Souza Segundo, *et al.*, Phys. Rev. Lett. **131**, 143801 (2023).
28. E. A. Gazazyan, A. V. Papoyan, D. Sarkisyan, and A. Weis, Laser Phys. Lett. **4**, 801–808 (2007).
29. A. Tonoyan, A. Sargsyan, E. Klinger, *et al.*, Eur. Phys. Lett. **121**, 53001 (2018).
30. T. Peyrot, C. Beurthe, S. Coumar, *et al.*, Opt. Lett. **44**, 1940 (2019).

FULL REFERENCES

1. D. Pizzey, J. D. Briscoe, F. D. Logue, *et al.*, "Laser spectroscopy of hot atomic vapours: from 'scope to theoretical fit," New J. Phys. **24**, 125001 (2022).
2. J. Kitching, "Chip-scale atomic devices," Appl. Phys. Rev. **5**, 031302 (2018).
3. A. Fabricant, I. Novikova, and G. Bison, "How to build a magnetometer with thermal atomic vapor: a tutorial," New J. Phys. **25**, 025001 (2023).
4. D. Uhland, H. Dillmann, Y. Wang, and I. Gerhardt, "How to build an optical filter with an atomic vapor cell," New J. Phys. **25**, 125001 (2023).
5. R. Finkelstein, S. Bali, O. Firstenberg, and I. Novikova, "A practical guide to electromagnetically induced transparency in atomic vapor," New J. Phys. **25**, 035001 (2023).
6. J. Miao, T. Shi, J. Zhang, and J. Chen, "Compact 459-nm cs cell optical frequency standard with $2.1 \times 10^{13}/\sqrt{\tau}$ short-term stability," Phys. Rev. Appl. **18**, 024034 (2022).
7. E. Klinger, A. Mursa, C. M. Rivera-Aguilar, *et al.*, "Sub-Doppler spectroscopy of the Cs atom 6S1/2–7P1/2 transition at 459 nm in a microfabricated vapor cell," Opt. Lett. **49**, 1953 (2024).
8. A. Damitz, G. Toh, E. Putney, *et al.*, "Measurement of the radial matrix elements for the $6s\,^2S_{1/2} \rightarrow 7p\,^2P_J$ transitions in cesium," Phys. Rev. A **99**, 062510 (2019).
9. G. Toh, N. Chalus, A. Burgess, *et al.*, "Measurement of the lifetimes of the $7p^2P_{3/2}$ and $7p^2P_{1/2}$ states of atomic cesium," Phys. Rev. A **100**, 052507 (2019).
10. M. Auzinsh, R. Ferber, F. Gahbauer, *et al.*, "Cascade coherence transfer and magneto-optical resonances at 455 nm excitation of cesium," Opt. Commun. **284**, 2863 (2011).
11. F. Li, B. Zhao, J. Wei, *et al.*, "Continuously tunable single-frequency 455 nm blue laser for high-state excitation transition of cesium," Opt. Lett. **44**, 3785 (2019).
12. G. Dutier, S. Saltiel, D. Bloch, and M. Ducloy, "Revisiting optical spectroscopy in a thin vapor cell: mixing of reflection and transmission as a fabry–perot microcavity effect," J. Opt. Soc. Am. B **20**, 793–800 (2003).
13. G. Dutier, A. Yarovitski, S. Saltiel, *et al.*, "Collapse and revival of a dicke-type coherent narrowing in a sub-micron thick vapor cell transmission spectroscopy," Europhys. Lett. **63**, 35 (2003).
14. D. Sarkisyan, T. Varzhapetyan, A. Sarkisyan, *et al.*, "Spectroscopy in an extremely thin vapor cell: Comparing the cell-length dependence in fluorescence and in absorption techniques," Phys. Rev. A **69**, 065802 (2004).
15. A. Sargsyan, G. Hakhumyan, A. Papoyan, *et al.*, "A novel approach to quantitative spectroscopy of atoms in a magnetic field and applications based on an atomic vapor cell with L = λ," Appl. Phys. Lett. **93**, 021119 (2008).
16. J.-M. Hartmann, X. Landsheere, C. Boulet, *et al.*, "Infrared look at the spectral effects of submicron confinements of co_2 gas," Phys. Rev. A **93**, 012516 (2016).
17. G. G. Arellano, J. C. de Aquino Carvalho, H. Mouhanna, *et al.*, "Probing molecules in gas cells of subwavelength thickness with high frequency resolution," Nat. Commun. **15**, 1862 (2024).
18. S. Briaudeau, D. Bloch, and M. Ducloy, "Detection of slow atoms in laser spectroscopy of a thin vapor film," Europhys. Lett. (EPL) **35**, 337–342 (1996).
19. J. Keaveney, A. Sargsyan, U. Krohn, *et al.*, "Cooperative Lamb Shift in an Atomic Vapor Layer of Nanometer Thickness," Phys. Rev. Lett. **108**, 173601 (2012).
20. A. Sargsyan, A. Amiryan, Y. Pashayan-Leroy, *et al.*, "Approach to quantitative spectroscopy of atomic vapor in optical nanocells," Opt. Lett. **44**, 5533–5536 (2019).
21. A. Laliotis, B.-S. Lu, M. Ducloy, and D. Wilkowski, "Atom-surface physics: A review," AVS Quantum Sci. **3** (2021).
22. M. Chevrollier, D. Bloch, G. Rahmat, and M. Ducloy, "Van der waals-induced spectral distortions in selective-reflection spectroscopy of cs vapor: the strong atom–surface interaction regime," Opt. Lett. **16**, 1879 (1991).
23. A. Sargsyan, R. Momier, C. Leroy, and D. Sarkisyan, "Competing van der waals and dipole-dipole interactions in optical nanocells at thicknesses below 100 nm," Phys. Lett. A **483**, 129069 (2023).
24. B. Dutta, J. C. d. A. Carvalho, G. Garcia-Arellano, *et al.*, "Effects of higher-order Casimir-Polder interactions on Rydberg atom spectroscopy," Phys. Rev. Res. **6**, L022035 (2024).
25. T. Peyrot, N. Šibalić, Y. R. P. Sortais, *et al.*, "Measurement of the atom-surface van der waals interaction by transmission spectroscopy in a wedged nanocell," Phys. Rev. A **100**, 022503 (2019).
26. C. S. Adams, J. D. Pritchard, and J. P. Shaffer, "Rydberg atom quantum technologies," J. Phys. B: At. Mol. Opt. Phys. **53**, 012002 (2019).
27. J. C. de Aquino Carvalho, I. Maurin, P. Chaves de Souza Segundo, *et al.*, "Spectrally sharp near-field thermal emission: Revealing some disagreements between a casimir-polder sensor and predictions from far-field emittance," Phys. Rev. Lett. **131**, 143801 (2023).
28. E. A. Gazazyan, A. V. Papoyan, D. Sarkisyan, and A. Weis, "Laser frequency stabilization using selective reflection from a vapor cell with a half-wavelength thickness," Laser Phys. Lett. **4**, 801–808 (2007).
29. A. Tonoyan, A. Sargsyan, E. Klinger, *et al.*, "Circular dichroism of magnetically induced transitions for D_2 lines of alkali atoms," Eur. Phys. Lett. **121**, 53001 (2018).
30. T. Peyrot, C. Beurthe, S. Coumar, *et al.*, "Fabrication and characterization of super-polished wedged borosilicate nano-cells," Opt. Lett. **44**, 1940–1943 (2019).